Catalysis Today 158 (2010) 415–422

Contents lists available at ScienceDirect

Catalysis Today

journal homepage: www.elsevier.com/locate/cattod

Comparison of catalytic combustion of carbon monoxide and formaldehyde over Au/ZrO_2 catalysts☆

Yong-Chun Hong[a], Ke-Qiang Sun[a], Ke-Hang Han[a], Gang Liu[b], Bo-Qing Xu[a,*]

[a] Innovative Catalysis Program, Key Lab of Organic Optoelectronics and Molecular Engineering, Department of Chemistry, Tsinghua University, Beijing 100084, China
[b] National Center for Nanoscience and Technology, Beijing 100190, China

ARTICLE INFO

Article history:
Available online 17 June 2010

Keywords:
Catalysis by gold
CO oxidation
Formaldehyde combustion
Induction period
Moisture effect
Zirconia

ABSTRACT

Catalytic combustion reactions of carbon monoxide and formaldehyde are compared over Au/ZrO_2 catalysts with varied Au loadings (0.25–4 wt%) and calcination temperatures (110–450 °C). The combustion of CO shows a distinct induction period over most catalysts while the reaction of HCHO proceeds steadily over every catalyst. Catalysts with varied calcination temperatures exhibit the same activity order in both reactions. The catalyst calcined at 200 °C appears to show the highest activity for either of the two reactions, suggesting that the amount of metallic Au and size of Au particles are crucial for both reactions. The mass specific activity (MSA) of Au in those catalysts calcined at 200 °C decreases with increasing Au loading for CO combustion but is almost independent of the Au loadings for HCHO combustion. Moisture (2000 ppm H_2O) addition to the gaseous feed of the CO combustion reaction eliminates the induction period, and the MSA of Au turns to be nearly constant and independent of the Au loadings. Possible reasons for the similarities/dissimilarities in gold catalysis for the combustion reactions of CO and HCHO are discussed.

1. Introduction

Since the discovery made by Haruta et al. [1] in 1987 that metal oxides supported Au nanoparticles can be extremely active for oxidative removal of poisonous CO from air, intensive research has been conducted worldwide to obtain in-depth understanding of this surprisingly active "inert" metal for both selective and complete oxidation (combustion) catalysis [2–6]. The CO oxidation or combustion reaction has long been the most investigated and "standard" reaction in heterogeneous oxidation catalysis involving supported transition metal catalysts like Pt and Pd. Although the nature of active gold for CO combustion still remains an issue of debate [6,7], oxygen activation in the CO combustion reaction is found rather different over supported Au nanoparticles from over those supported transition metal catalysts. Abundant knowledge has been accumulated about the effects of gold particle size [4,8] and oxidation state [15,17,18,21–23], Au–support interaction [14], feed moisture [23–26] and also others [6]. The combustion of formaldehyde (HCHO), a popular poisonous molecule [28] bearing similar structure to CO, is another important reaction for air cleaning. However, little is known about the performance and nature of active site in supported Au catalyst for HCHO combustion [9,10,29–37], which is in strong contrast to the enthusiasm on the CO combustion reaction.

Au/ZrO_2 catalyst was extensively investigated both in catalytic oxidation and hydrogenation reactions [11–13]. Earlier reports from this laboratory have shown that Au/ZrO_2 catalysts prepared by deposition–precipitation with ammonia (DPA) were remarkably active towards CO combustion [14,17], 1,3-butadiene hydrogenation [16,17] and selective hydrogenation of the nitro in chloronitrobenzenes [19]. Co-existence of metallic and cationic gold (Au^{3+}) in a proper ratio was found superior to "purely" metallic Au for the CO combustion reaction [17], while isolated surface Au^{3+} sites were identified most active for selective 1,3-butadiene hydrogenation to form butenes [16,17]. Interestingly, the nanosize of ZrO_2 "support" or size-match between Au and ZrO_2 nanoparticles was shown also critical to the activity for the CO combustion reaction [14].

Herein, Au/ZrO_2 catalysts prepared by deposition–precipitation with urea (DPU), which enabled formation of smaller Au particles compared with those prepared by DPA in Refs. [14,17], are used to catalyze the combustion reactions of CO and HCHO. Systematic investigation on the effects of calcination temperature, Au loading and moisture in reaction feed has been made in attempts to establish relationship between the gold catalysis for the two reactions.

☆ 7th Asia Pacific Conference on Sustainable Energy & Environmental Technologies (APCSEET 2009).

* Corresponding author. Tel.: +86 10 6279 2122; fax: +86 10 6279 2122.
E-mail address: bqxu@mail.tsinghua.edu.cn (B.-Q. Xu).

0920-5861/$ – see front matter © 2010 Elsevier B.V. All rights reserved.
doi:10.1016/j.cattod.2010.05.017

2. Experimental

2.1. Chemicals

$HAuCl_4{\cdot}4H_2O$ was obtained from Guiyang Institute of Precious Metals (Guizhou, China). Urea, polyformaldehyde and $ZrO(NO_3)_2{\cdot}2H_2O$ were purchased from Beijing Chemical Reagent Company. These chemicals were in the analytical grade (AR) and were used as-received.

2.2. Preparation of Au/ZrO_2 catalysts

ZrO_2 with a BET surface area of 129 $m^2\,g^{-1}$ was prepared by thermal treatment of a $ZrO(OH)_2$ alcogel in flowing nitrogen (60 mL min^{-1}) at 450 °C for 5 h. The alcogel was obtained by washing a conventional $ZrO(OH)_2$ hydrogel with anhydrous ethanol. Except that $ZrO(NO_3)_2{\cdot}2H_2O$ was employed instead of $ZrOCl_2{\cdot}8H_2O$ as the precursor of zirconium, the present preparation of the $ZrO(OH)_2$ hydrogel followed the same procedure as detailed previously [20]. This change of the zirconium precursor was made intentionally because chloride ions were commonly considered poisonous to Au catalysis [6].

Au/ZrO_2 samples with various gold loadings (0.25–4.0 wt%) were prepared by deposition–precipitation with urea [27]. In the preparation of 1 wt% Au/ZrO_2 sample, 2 mL of $HAuCl_4$ solution (10 mg_{Au} mL^{-1}), 2.44 g of urea (urea/Au = 400, molar ratio), 1.98 g of the as-prepared ZrO_2 powders (mesh size: >100) and 50 mL of deionized water were added into a three-neck flask jacketed with a circulating water bath thermostated at 80 °C, and the flask was covered with a opaque package to keep off the room light. The suspensions were then stirred vigorously for 6 h (final pH = ca. 7.6), followed by overnight aging at room temperature. The solid was filtered and washed extensively with deionized water until it was free of chloride ions (i.e., until conductance of the filtrate was below 10^{-5} S m^{-1}). The filter residue was then dried at 110 °C for 5 h and calcined at different temperatures (200–450 °C) in flowing air (60 mL min^{-1}) for 5 h. The samples are denoted as "*m*Au/ZrO_2-*T*" where *m* is the Au loading (wt%) and *T* the calcination temperature (°C). All samples were stored at −18 °C in a refrigerator with 5A molecular sieve to prevent possible deterioration during storage [18].

2.3. Characterizations

The actual Au loading in each catalyst sample was determined by ICP-AES analysis. BET measurements were carried out with N_2 adsorption at −196 °C on a Micromeritics ASAP 2010C instrument after the samples were degassed at 200 °C for 2 h. High-angle annular dark-field scanning transmission electron microscopy (HAADF-STEM) measurements were performed on a Tecnai G2 F20 U-Twin system operating at 200 kV. X-ray diffraction (XRD) patterns were recorded on a Bruker D8 Advance X-ray diffractometer with a Ni-filtered Cu-K_α (incident wavelength = 0.15406 nm) radiation source at 40 kV and 40 mA, the scan rate is 4° min^{-1}.

2.4. Catalytic reactions

The catalytic CO and HCHO combustion reactions were performed in continuous flow, fixed-bed U-shaped quartz reactors (i.d. 4 mm) under atmospheric pressure (0.1 MPa). Unless otherwise specified, the catalyst (50 mg) diluted with quartz sand (100 mg) was *in situ* pretreated with a synthetic air at 200 °C for 1 h and then cooled down to the reaction temperature. The *in situ* pretreatment temperature was 110 °C when those catalyst samples dried at 110 °C but with no further calcination at higher temperatures were used for the reactions. In order to eliminate the effect of tubing dead-volume, analysis of the reactor effluents was not made in the initial 5 min from the start of both reactions.

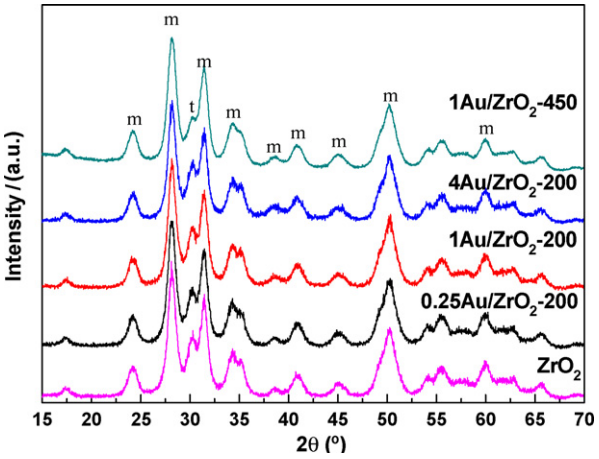

Fig. 1. XRD patterns of ZrO_2 and Au/ZrO_2 samples. The marks refer to diffraction peaks for the monoclinic (m) and tetragonal (t) phases, respectively.

For the CO combustion reaction, the reaction gas (1 vol% CO in synthetic air) was introduced with a total space velocity (GHSV) of 33,600 mL h^{-1} g cat^{-1} into the reactor thermostated at 0 °C in a water–ice mixture. The reactor effluent was on-line analyzed with an HP-6890 gas chromatograph equipped with a molecular 5A column and a thermal conductivity detector (TCD).

For HCHO combustion, the reaction gas (3000 ppm HCHO in synthetic air) was introduced with a total GHSV of 60,000 mL h^{-1} g cat^{-1} into the reactor by having the synthetic air flow through a polyformaldehyde reservoir thermostated at 50 °C for HCHO generation. This setup can provide dry HCHO with a stable concentration (3000 ppm HCHO at 50 °C) and is of advantageous compared with the frequently used approach using formalin for HCHO generation [10,29–31,33–37], which would result in unsteady water (moisture) co-feeding and thus variation in the inlet HCHO concentration during the reaction. The reactor effluent was on-line analyzed with a GC 122 chromatograph (Shanghai Analytical Apparatus Corporation, China), which was equipped with a molecular 5A column, a catalytic methanation converter and a flame ionization detector (FID). The reaction temperature was kept above 60 °C to avoid any condensation of HCHO in the reactor. The inlet and outlet tubings from the reactor were thermostated at 120 °C to prevent possible polymerization of HCHO.

3. Results

3.1. Physical properties of Au/ZrO_2 catalysts

The actual Au loadings of Au/ZrO_2 samples were determined by ICP-AES analysis and the deposition efficiency of gold (i.e., actual-to-theoretical Au loading) was always near 100% in every DPU preparation of the samples. Fig. 1 shows the XRD patterns of ZrO_2 and *m*Au/ZrO_2-*T* samples. ZrO_2 in all samples appeared as polycrystallines containing both monoclinic (JCPDS card 37-1484) and tetragonal (JCPDS card 50-1089) phases. The XRD patterns of *m*Au/ZrO_2-*T* samples were very similar to that of ZrO_2 without gold and were independent of both *m* and *T*, indicating that the Au loading and calcinations during the catalyst preparation had little effect on the phase structure and composition of ZrO_2 crystals [16,17]. The presence of small Au crystallites was uncertain in the XRD patterns of *m*Au/ZrO_2-*T* samples since the most possible diffraction signal for Au crystallites, which would show up at $2\theta = 38.2°$ (for Au(1 1 1)), could be overlapped by the signals for monoclinic ZrO_2 at $2\theta = 38.4$ and 38.5°. However, the consistent silence of Au particles in every

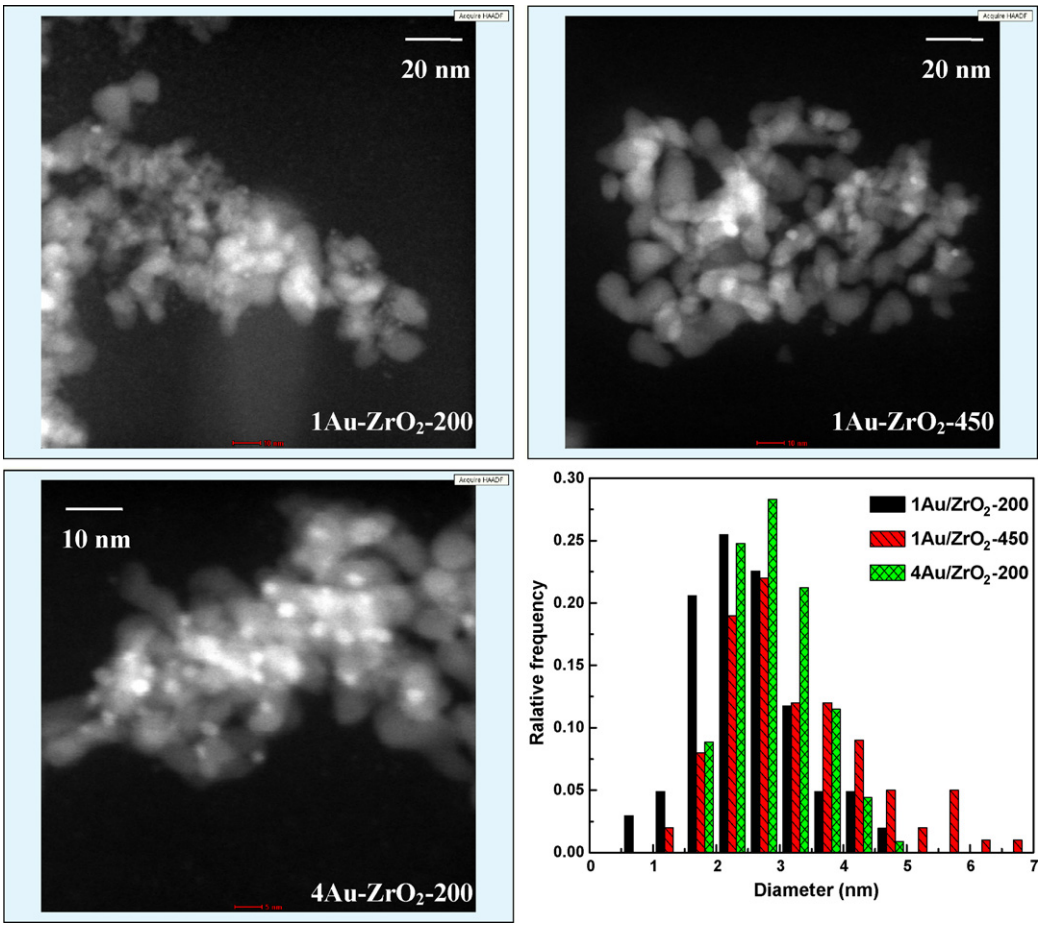

Fig. 2. Representative HAADF-STEM micrographs of *m*Au/ZrO_2-*T* catalysts. The bar graph shows the corresponding size distribution of Au particles.

XRD pattern in Fig. 1 would suggest that Au particles bigger than 5 nm were of insignificance.

Representative HAADF-STEM micrographs of *m*Au/ZrO_2-*T* samples are presented in Fig. 2. Metallic Au was characterized as well dispersed small particles whose sizes were carefully measured by variation of the magnification. The bar graph in Fig. 2 shows the corresponding size distribution of metallic Au particles. The average Au particle size was 2.5 nm in 1Au/ZrO_2-200 and 2.8 nm in 4Au/ZrO_2-200 sample, indicating that the increase of Au loading has only a slight influence on Au size distribution in the samples when the calcination temperature was $T = 200\,^{\circ}C$. However, the average Au particle size in 1Au/ZrO_2-450 (3.4 nm) was significantly larger than that in 1Au/ZrO_2-200 sample (2.5 nm), indicating a significant sintering of the Au particles when the catalyst calcination temperature *T* was raised from 200 to 450 °C. For the sample loaded with the least Au (i.e., 0.25Au/ZrO_2-200), we detected no metallic Au particle.

The BET surface area, pore volume, particle size and phase composition of ZrO_2 in *m*Au/ZrO_2-*T* samples are listed in Table 1. The surface area was lowered by 17% for 4Au/ZrO_2-200 and 25% for 1Au/ZrO_2-450 sample, compared with that of the "pure" ZrO_2. Such changes in the sample surface area could be arisen from a blocking by Au particles of some pores in the starting ZrO_2 support since the calcination temperature of *m*Au/ZrO_2-*T* was kept no higher than that of the support material (450 °C). The sizes of ZrO_2 particles, as indicated by the average crystallite sizes derived from the XRD patterns as well as the particle sizes from the TEM measurements, remained unchanged throughout the catalyst preparation process (DPU and the following drying and calcination). Phase composition of the ZrO_2 support as shown in the last column of Table 1 was also not changed during the catalyst preparation.

3.2. Catalytic performance of Au/ZrO_2 for the combustion of CO and HCHO

3.2.1. Effect of the catalyst calcination temperature

Fig. 3 shows the catalytic performance of 1Au/ZrO_2-*T* catalysts for the CO combustion at 0 °C by plotting the CO conversion against the reaction time-on-stream (TOS). An induction period was clearly seen for every catalyst except 1Au/ZrO_2-450 ($T = 450\,^{\circ}C$), which produced the lowest CO conversion (ca. 1%). The induction period over the as-dried 1Au/ZrO_2-110 catalyst ($T = 110\,^{\circ}C$) evolved slowly and extended to 18–20 h when the CO conversion level reached at 15%. The induction period was shortened to 3–4 h by increasing the catalyst calcination temperature (*T*) to 200 and 300 °C. The steady CO conversion level (i.e., after the induction period) reached 45% at $T = 200\,^{\circ}C$ (1Au/ZrO_2-200) but was then lowered to 20% at $T = 300\,^{\circ}C$ (1Au/ZrO_2-300).

A further comparison of the 1Au/ZrO_2-110 and 1Au/ZrO_2-450 catalysts was made by increasing the reaction temperature to 60 °C for CO combustion. As is shown in Fig. 4, the 1Au/ZrO_2-450 catalyst featured again a much lower activity and no induction period. In contrast, the activity of 1Au/ZrO_2-110 catalyst developed steeply in the initial 15 min and the induction period extended to longer than 3 h, during which the CO conversion increased to a level of ca. 80%.

In a separate experiment, the CO combustion reaction over 1Au/ZrO_2-110 catalyst was carried out by changing the reaction temperature between 60 and 0 °C. Fig. 5 presents the results of this experiment. The CO conversion level increased clearly in the second event at both temperatures although it basically remained unchanged at 0 °C in every event. The continued increase in CO

Table 1
Textural properties of ZrO_2 and Au/ZrO_2 samples.

Sample	BET surface area (m^2/g)	Pore volume[a] (cm^3/g)	ZrO_2 size (nm)		ZrO_2 phase[b]
			XLBA[c]	TEM[d]	
ZrO_2	129	0.35	M9/T9	11.8 ± 3.2	M85/T15
$1Au/ZrO_2$-200	115	0.34	M9/T9	11.4 ± 3.2	M85/T15
$1Au/ZrO_2$-450	97	0.31	M8/T9	11.4 ± 2.6	M89/T11
$4Au/ZrO_2$-200	107	0.29	M9/T9	11.6 ± 3.1	M84/T16

[a] Obtained from desorption branch using the BJH method.
[b] Percentage of the monoclinic phase $= 1.6I_{M(\bar{1}\,1\,1)}/(1.6I_{M(\bar{1}\,1\,1)} + I_{T(1\,1\,1)})$; percentage of the tetragonal phase $= I_{T(1\,1\,1)}/(1.6I_{M(\bar{1}\,1\,1)} + I_{T(1\,1\,1)})$.
[c] Calculated according to the well-known Scherrer equation using the $(\bar{1}\ 1\ 1)$ diffraction ($2\theta = 28.5^\circ$) for monoclinic (M) and the $(1\ 1\ 1)$ diffraction ($2\theta = 30.4^\circ$) for tetragonal (T) zirconia crystallites.
[d] At least 200 particles were randomly measured to determine the mean diameter of ZrO_2 particles according to equation $d = \sum n_i d_i / \sum n_i$, where n_i and d_i are the number and diameter of ZrO_2 particles, respectively.

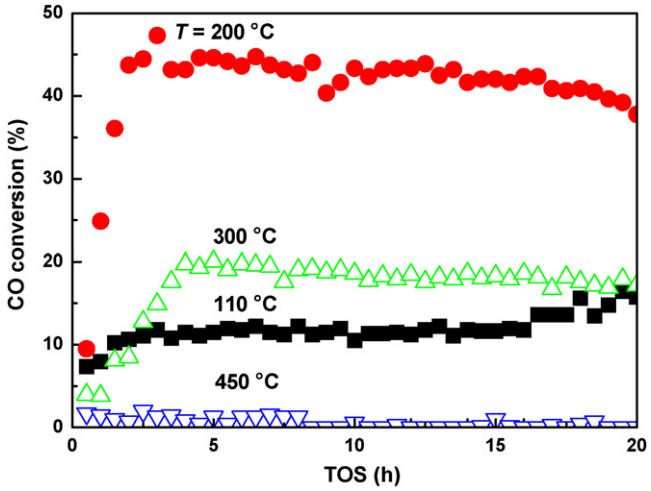

Fig. 3. Performance of $1Au/ZrO_2$-T catalyst for CO conversion at 0 °C. The marks show the catalyst calcination temperature T.

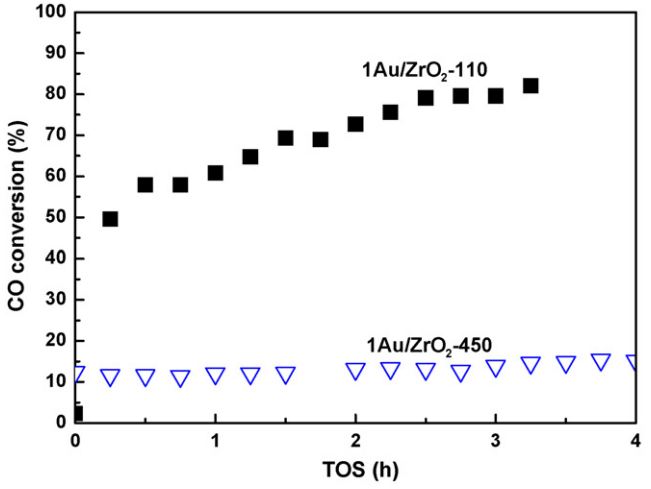

Fig. 4. CO combustion over $1Au/ZrO_2$-110 and $1Au/ZrO_2$-450 catalysts at 60 °C.

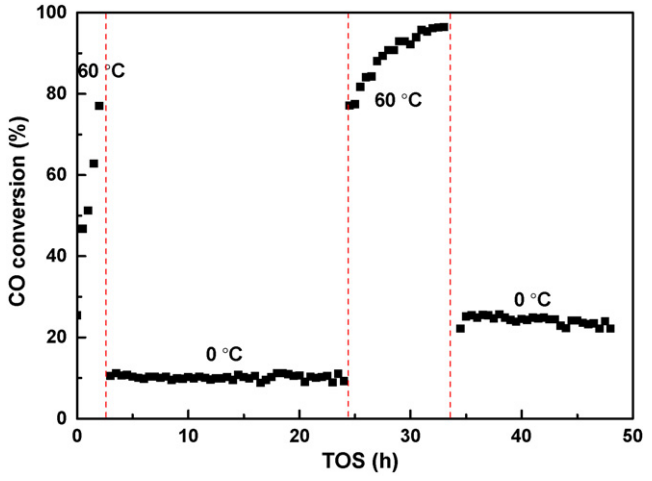

Fig. 5. Performance of $1Au/ZrO_2$-110 catalyst for CO combustion by variation of the reaction temperature.

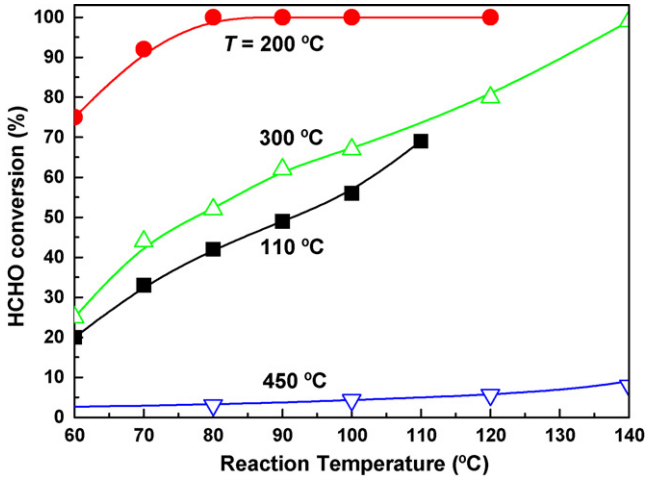

Fig. 6. Effect of reaction temperature on HCHO conversion over $1Au/ZrO_2$-T catalysts. The marks show the catalyst calcination temperature T.

conversion level in the second event at 60 °C demonstrates lively a continued evolution of the induction period at this temperature. Nearly complete removal of CO by the combustion reaction can apparently be made possible at 60 °C when this $1Au/ZrO_2$-110 catalyst was subject to a sufficient activity development, though the space velocity of the gas feed was as high as 33,600 mL h^{-1} g cat^{-1} in this study. These results also suggest that the length of the induction period would be dependent of the reaction temperature.

The combustion of HCHO under isothermal reaction conditions was characterized by a reasonably stable HCHO conversion over every $m Au/ZrO_2$-T catalyst; no induction period was observed for this combustion reaction. Fig. 6 shows the catalytic performance of $1Au/ZrO_2$-T catalysts for the combustion of HCHO at different temperatures. The HCHO conversion level at each reaction temperature was shown as the averaged conversion data during a reaction period of 2 h. It is apparent that the catalyst calcination temperature T has a significant effect on its activity for HCHO combustion. The

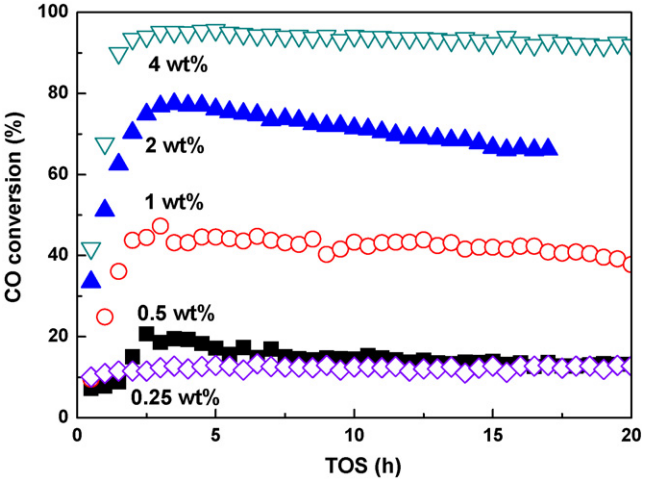

Fig. 7. Performance of mAu/ZrO_2-200 catalysts for CO combustion at 0 °C.

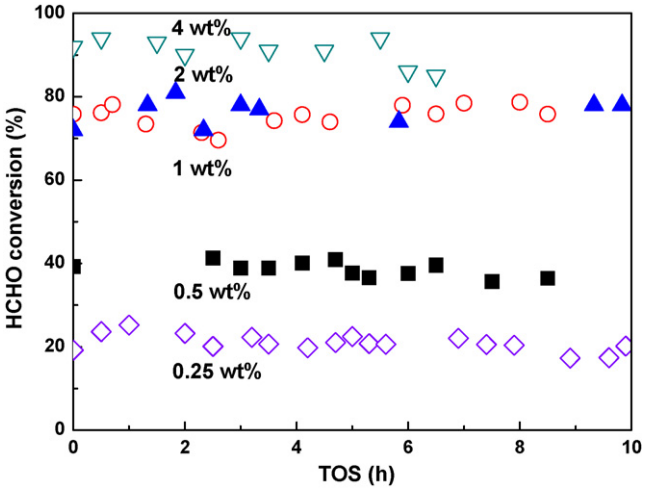

Fig. 8. Performance of mAu/ZrO_2-200 catalysts for HCHO combustion at 60 °C.

catalyst of T = 200 °C (1Au/ZrO_2-200) induced a HCHO conversion as high as 75% at 60 °C while the one of T = 450 °C (1Au/ZrO_2-450) effected almost no HCHO conversion at the same temperature. The HCHO conversion was 20% and 25%, respectively, over the other two catalysts of T = 110 and 300 °C. Therefore, the catalyst activity order for the HCHO combustion reaction is 1Au/ZrO_2-200 > 1Au/ZrO_2-300 > 1Au/ZrO_2-110 > 1Au/ZrO_2-450. This order agrees with that of the same catalysts for the CO combustion reaction at 0 °C, as shown in Fig. 3.

3.2.2. *Effect of Au loading*

The effect of Au loading on the two combustion reactions was studied by fixing the catalyst calcination temperature at T = 200 °C and varying the Au loading in the range of 0.25–4.0 wt%. The performance of these mAu/ZrO_2-200 catalysts for the CO combustion reaction at 0 °C is shown in Fig. 7. A distinct induction period of 3–5 h was seen again, irrespective of the Au loadings. The CO conversion level increased with increasing the Au loading of the catalyst except for m = 0.25 and 0.5 wt% Au, these two catalysts effected very similar CO conversion levels after their induction periods. The eightfold increments in Au loading from 0.5 to 4.0 wt% enhanced the CO conversion level by sixfold (from 15% to 95%).

Fig. 8 shows the performance of mAu/ZrO_2-200 catalysts for the combustion of HCHO at 60 °C. No induction period was observed over all of these catalysts. As it was already seen in the CO combustion reaction (Fig. 7), the conversion of HCHO also increased, from 20% to 90%, with increasing the Au loading. Interestingly, a doubling of the Au loading from 1 to 2 wt% Au had little effect on HCHO conversion but the doubling from 0.25 to 0.5 wt% Au nearly doubled the HCHO conversion level, which are distinctive from their behavior in the CO combustion reaction.

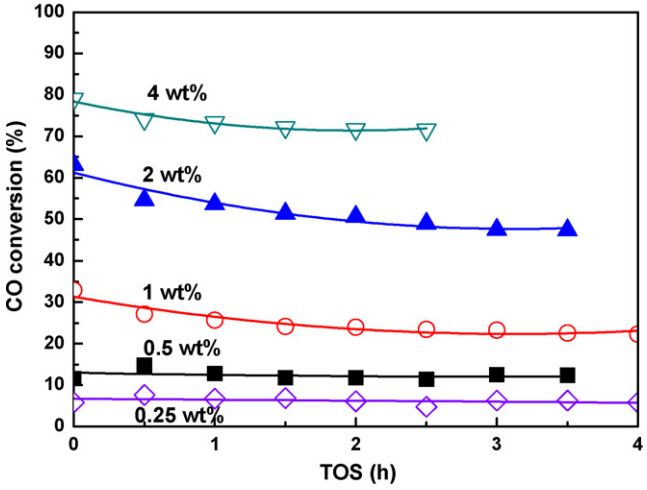

Fig. 9. CO combustion at 0 °C over mAu/ZrO_2-200 catalysts in the presence of moisture (2000 ppm H_2O).

Since the combustion reaction of either CO or HCHO is exothermal, reactant conversion levels higher than 50% during both reactions could result in significant temperature jump, even when the catalysts were diluted with quartz sand as in this study. In order to make assessment to the "real" activity, we evaluated the mass specific activity (MSA) and turnover frequency (TOF) of Au in each catalyst by setting 15% for the up limit to the CO conversion and 40% to the HCHO conversion for the combustion reactions. These kinds of catalytic reaction data were measured by increasing the space velocity (or reducing the contact time with the catalyst) of the reactant. Table 2 reports the activity data by MSA and TOF of Au in mAu/ZrO_2-200 catalysts. The MSA data for the combustion reaction of CO decreased with increasing the Au loading but, very surprisingly, the change in the Au loading did not alter the MSA data for the combustion reaction of HCHO. Thus, the relative activity by MSA of Au for the CO combustion reaction to that for the HCHO combustion (i.e., MSA_R), shown in the last column of Table 2, also decreased with increasing the Au loading.

Table 3 compares the activity data of the present Au/ZrO_2 catalysts for the combustion of HCHO with those different catalysts published in recent literature. It should be noted that the present Au/ZrO_2 catalysts can be regarded as the most active catalysts, including also supported Pt and Pd catalysts [9], for the removal of HCHO from air by catalytic combustion.

3.2.3. *Effect of moisture on CO combustion*

One of the major differences between CO and HCHO combustion is that H_2O is a must product of the HCHO combustion. Moisture (H_2O) would be produced at a level of 1500 ppm if the HCHO conversion level reached 50% during the combustion of HCHO in this present work. In contrast, the moisture residue would be lower than 10 ppm in the reactant gas feed of the CO combustion reaction under "dry" condition. It has already been known that a presence of moisture would strongly affect the catalysis of Au in the CO combustion [23–26]. In order to gain an insight into the moisture effect on the present Au/ZrO_2 catalysts, 2000 ppm H_2O was added to the CO combustion reactor by passing the reaction feed gas through a bubbling reservoir filled with a saturated aqueous solution of NaCl and thermostated with a NaCl-ice bath at ca. −20 °C.

Table 2
Activities of Au/ZrO_2 catalysts.

Sample	Au size[a] (nm)	CO oxidation (0 °C)		HCHO oxidation (60 °C)		MSA_R[b]
		MSA[c] (10^{-5} mol s^{-1} g_{Au}^{-1})	TOF[d] (10^{-2} s^{-1})	MSA[e] (10^{-5} mol s^{-1} g_{Au}^{-1}))	TOF (10^{-2} s^{-1})	
0.25Au/ZrO_2-200	n.d.[f]	20.7 (10.7)	–	9.3	–	2.2 (1.2)
0.5Au/ZrO_2-200	n.m.[g]	12.5 (10.5)	–	8.6	–	1.5 (1.2)
1Au/ZrO_2-200	2.5 ± 0.8	10.8 (10.1)	4.2 (3.9)	8.9	3.4	1.2 (1.1)
2Au/ZrO_2-200	n.m.	9.3 (10.6)	–	9.2	–	1.0 (1.2)
4Au/ZrO_2-200	2.8 ± 0.7	8.2 (10.0)	3.4 (4.1)	9.2	3.9	0.9 (1.1)
1Au/ZrO_2-450	3.4 ± 1.3	0.2	0.1	0	0	–

[a] At least 100 particles were randomly measured to determine the mean diameter of Au particles according to the equation $d = \sum n_i d_i / \sum n_i$, where n_i and d_i are the number and diameter of Au particles, respectively.
[b] MSA_R = (MSA for CO combustion)/(MSA for HCHO combustion). Numbers in parentheses are obtained using the CO combustion rates measured under the moist condition (2000 ppm H_2O).
[c] The mass specific activity (MSA) data were obtained at the reactant conversion levels lower than 15% by reducing the contact time. Data in parentheses refer to those obtained under moist condition (2000 ppm of H_2O).
[d] The turnover frequency (TOF) data were calculated based on the average Au particle size, assuming closed-shell Au particles of nearly spherical shape [6]. Data in parentheses refer to those obtained under moist condition (2000 ppm of H_2O).
[e] Obtained at HCHO conversion levels lower than 40% by reducing the contact time.
[f] Not detected by HAADF-STEM.
[g] Not measured.

Table 3
Comparison with the literature data on HCHO combustion over supported gold and other metal catalysts.

Sample[a]	Rxn. temp. (°C)	C_{HCHO} (ppm)	Conv. (%)	MSA[b] (10^{-5} mol s^{-1} g_{metal}^{-1})	Ref.
0.25Au/ZrO_2-DPU	60	3000	21	9.3	This work
4Au/ZrO_2-DPU	60	3000	33	9.2	This work
1Au/α-Fe_2O_3-CP	ca. 55[c]	5000	50	6.2	9
1Pt/γ-Al_2O_3	ca. 55	5000	50	6.2	9
1Pd/γ-Al_2O_3	ca. 55	5000	50	6.2	9
1Au/TiO_2-IM	ca. 70	100	ca. 15	0.09	10
1Pd/TiO_2-IM	ca. 62	100	ca. 22	0.14	10
1Rh/TiO_2-IM	ca. 62	100	ca. 77	0.49	10
0.42Au/MgO-CD	ca. 135	3000	ca. 8	6.9	32
0.38Au/γ-Al_2O_3-CD	ca. 135	3000	ca. 10	9.6	32
0.29Au/TiO_2-CD	ca. 60	3000	ca. 5	6.3	32
0.23Au/CeO_2-CD	ca. 60	3000	ca. 10	16	32
0.41Au/TiO_2-DP	30	450	ca. 20	0.41	34
0.67Au/α-Fe_2O_3-CP	50	600	50	2.9	35
0.71Au/α-Fe_2O_3-IM	75	600	50	2.7	35
0.42Au/CeO_2-DP	ca. 53	600	ca. 32	3.7	36
0.85Au/ZrO_2	ca. 60	67.2	ca. 20	0.10	37

[a] Samples are noted as "*x*Metal/Support-Preparation Method" where *x* is metal loading (wt%), DPU for deposition–precipitation with urea, CP for co-precipitation, IM for impregnation, CD for colloid deposition, and DP for deposition–precipitation.
[b] Mass specific activity (MSA) was calculated from data obtained at reaction temperature comparable to 60 °C (reaction temperature used in this work) or at low HCHO conversion level (less than 50%).
[c] With uncertainty for reading data from figures.

Fig. 9 shows the reaction time courses of each *m*Au/ZrO_2-200 catalyst for the CO combustion reaction under the presence of 2000 ppm moisture. A comparison of the data in Fig. 9 with those in Fig. 7 clearly indicates that the presence of moisture resulted in elimination of the induction period of the CO combustion reaction observed under the "dry" condition (Fig. 7). The catalyst activity data by MSA of Au were again measured at CO conversion levels lower than 15% under the moist condition, which are also reported in Table 2 for comparison with those measured under the "dry" condition. The MSA data of 0.25Au/ZrO_2-200 and 0.5Au/ZrO_2-200 catalysts decreased and that of 1Au/ZrO_2-200 unchanged but that of 2Au/ZrO_2-200 and 4Au/ZrO_2-200 even increased slightly as compared with those measured under the "dry" condition. Consequently, the MSA data of Au in these *m*Au/ZrO_2-200 catalysts became close (ca. 10×10^{-5} mol s^{-1} $g_{Au}{}^{-1}$) for the CO combustion reaction under the moist condition. Thus, the relative activity by parameter MSA_R became almost invariant (Table 2).

4. Discussion

This work provides the first comparison of Au catalysis for the removal of CO and HCHO from air by catalytic combustion. The most important difference observed between these two combustion reactions was that the *m*Au/ZrO_2-*T* catalysts of $T \leq 300$ °C showed consistently a distinct induction period in the early stage of the CO combustion reaction under the "dry" condition but their catalysis for the combustion of HCHO proceeded steadily without any induction period. However, the catalytic performance of these same catalysts for the CO combustion reaction under the moist condition (i.e., when 2000 ppm H_2O was added to the reacting gas feed) was found very similar to their performance for the combustion of HCHO. These results would indicate that the active gold sites for the HCHO combustion reaction are closely related with those active for the combustion of CO under the moist condition.

It has been frequently shown [2,15,21–23] that small metallic Au particles are crucial for the CO combustion/oxidation catalysis. According to Haruta [2], Au particles with sizes less than ca. 5 nm are the key to efficient CO combustion catalysis. Smaller Au particles would generally show higher MSA numbers [4,8]. However, a complete reduction of cationic gold species in the supported catalysts would usually require calcinations of the catalysts at a temperature no lower than 400 °C, which could also induce significant Au sintering [14,16,33,35]. The unreduced cationic gold species in the final catalysts would in turn affect the activity and sta-

bility of the co-existing metallic Au particles for the CO combustion reaction [5,7,15,17].

The induction period observed in the CO combustion reaction under the "dry" condition was strongly associated with the catalyst calcination temperature T (Figs. 3 and 4). According to our earlier work [16,17], this temperature T would determine the percentage of cationic gold species in mAu/ZrO_2-T catalysts. The content of cationic gold in the 1Au/ZrO_2-T samples of T = 200, 300 and 450 °C would be ranked in the order of 1Au/ZrO_2-200 > 1Au/ZrO_2-300 > 1Au/ZrO_2-450. The induction period was the most prominent over 1Au/ZrO_2-200 and less prominent over 1Au/ZrO_2-300. The content of cationic gold in the 1Au/ZrO_2-450 sample should be zero since the high temperature calcination (T = 450 °C) could assure a complete reduction of the cationic gold to form metallic Au particles [6,16,17]. The CO combustion reaction conducted over this 1Au/ZrO_2-450 catalyst showed no induction period both at 0 and 60 °C (Figs. 3 and 4). These observations directly relate the induction period with the remaining unreduced cationic gold in the catalyst samples [15,21–23]. We thus have enough reason to associate the induction period with a continued reduction of the remaining cationic gold to form metallic Au particles that are active for the CO combustion reaction.

The induction period was least obvious at 0 °C over the 1Au/ZrO_2-110 sample (Fig. 3) in which cationic gold species would prevail [16,17]. This could be due to a very slow reduction rate of the cationic gold species at such a low reaction temperature. According to Kung and co-workers [15], metallic Au could function as the catalyst for the reduction of cationic gold species by CO at 0 °C. Thus, the lack of metallic Au in the 1Au/ZrO_2-110 sample should be responsible for the least obvious induction period over the 1Au/ZrO_2-110 catalyst in Fig. 3. This explanation is strongly supported by the distinctly detected induction period over the same 1Au/ZrO_2-110 catalyst in Figs. 4 and 5 when the reaction temperature was raised to 60 °C to induce easier reduction of the cationic gold species. In contrast, the CO combustion reaction over the 1Au/ZrO_2-450 catalyst at 60 °C had also no induction period (Fig. 4), which further corroborates that the reduction of cationic gold species is responsible for the induction period in the CO oxidation catalysis under the "dry" condition.

The most important finding of this work would be that the addition of 2000 ppm H_2O to the reacting gas mixture can eliminate the distinct induction period of the CO combustion reaction over mAu/ZrO_2-200 catalysts. This elimination of the reaction induction period also uncovered the similarity in gold catalysis for the combustion reactions of CO and HCHO over the mAu/ZrO_2-200 catalysts (Figs. 8 and 9 and Table 2). The MSA of Au in the CO combustion reaction decreased more or less with increasing the Au loading under the "dry" condition but changed little under the moist condition. This dramatic change in the catalyst performance indicates that the added moisture changed the nature and/or amount of active sites for the CO combustion reaction. Multiple functions of moisture (H_2O) in Au-catalyzed CO combustion reaction were reported in the literature [18,23–26]. A low concentration of moisture (ca. 200 ppm) could effect positively by H_2O-assisted activation of oxygen and removal of surface carbonate species while a high concentration of H_2O (e.g., 6000 ppm) could effect negatively by blocking the catalytically active sites [25,26]. The moisture could also promote *in situ* CO reduction of cationic gold species [23,24]. We showed very recently that residual H_2O in freshly prepared Au/TiO_2 samples can promote the reduction of Au^{3+} and induce agglomeration of metallic Au particles even during storage under ambient conditions [18]. For those catalysts that showed prominent induction periods in the CO combustion reaction under the "dry" condition (Fig. 7), the catalytic CO combustion rates at the initial stage of the reaction under the moist condition (Fig. 9) were even significantly higher. These remarkable increments in the CO combustion rates indicate that the elimination of the induction period by the addition of 2000 ppm H_2O would be accounted for by a H_2O-promoted rapid reduction of the cationic gold species. This kind of reduction chemistry proceeded so quickly that it became completed or equilibrated by the moment when the reactor outlet gas was sampled for the first time, i.e., in less than 5 min from the start of the reaction. The so-called H_2O-assisted activation of oxygen [25,26] did not operate in the present reaction systems since the MSA data of Au measured under the moist condition for the 1Au/ZrO_2-200 and 2Au/ZrO_2-200 catalysts were very close to those obtained after the induction periods under the "dry" condition. The remarkable activity loss of 0.25Au/ZrO_2-200 and 0.5Au/ZrO_2-200 catalysts could be due to H_2O-promoted agglomeration of very small metallic Au particles, a point which we addressed very recently on freshly prepared Au/TiO_2 samples [18].

Small metallic Au particles are also crucial for the combustion reaction of HCHO [30,33–36]. The decrease in the catalytic rate of 1Au/ZrO_2-T catalysts with T increasing from 200 to 450 °C for the HCHO combustion reaction could be mainly due to growth of the Au particles (Fig. 2 and Table 2), similar consideration was presented earlier to account for the calcination temperature effects of Au/CeO_2 and Au/Fe_2O_3 catalysts on their catalytic activity also for the combustion of HCHO [30,35,36].

The most significant difference observed between the CO and HCHO combustion reactions is that the combustion of HCHO proceeded with no induction period. Except of this, the two combustion reactions resembled each other over the present mAu/ZrO_2-T catalysts. Because H_2O is a must product of the HCHO combustion reaction (e.g., 1500 ppm H_2O would be produced when a half of the HCHO reactant became combusted) and the reaction temperature for the combustion of HCHO was set significantly higher than that for the combustion of CO (60 °C versus 0 °C), H_2O-promoted reduction of the remaining unreduced gold cations would easily occur, using HCHO and/or its derived reaction intermediates including CO [10] as the reactant. This argument is well supported by the similarity of the HCHO combustion reaction to the CO combustion reaction under the moist condition but not the "dry" condition. *In situ* reduction of cationic gold during HCHO combustion reaction over Au/CeO_2 [36] and Au/ZrO_2 [37] catalyst was detected by *ex situ* XPS characterization. The invariant relative activity data that are shown as MSA_R in the brackets of the last column in Table 2 would be an indication that the catalysis by Au in the CO combustion reaction under the moist condition also operates in the HCHO combustion reaction.

The above discussion is made with no consideration of any possibility for a presence of un-reducible cationic gold in our Au/ZrO_2 catalysts during the HCHO combustion reaction as well as during the CO combustion reaction under the moist condition or after the induction period under the "dry" condition. There is evidence in the literature showing that some co-existing cationic gold species could enhance the activity of supported Au catalysts for the CO combustion reaction [5–7,15,17]. This issue remains open for further investigation.

5. Conclusions

This work is the first to compare Au catalysis in the combustion reactions of CO and HCHO. The most important difference observed between the two combustion reactions was that the mAu/ZrO_2-T catalysts of $T \leq 300$ °C showed consistently a distinct induction period in the early stage of the CO combustion reaction under the "dry" condition but their catalysis for the combustion of HCHO proceeded steadily without any induction period. The concentration of unreduced cationic gold in the fresh catalyst determined the prominent of the induction period. Addition of 2000 ppm H_2O to the

reacting gas feed eliminated the induction period of the CO combustion reaction, due to a rapid H_2O-promoted reduction of the cationic gold. The catalytic performance of Au/ZrO_2 catalysts for the CO combustion reaction under this moist condition closely resembled that for the HCHO combustion reaction. These data demonstrate that gold active sites for the combustion of HCHO are associated closely with those for the combustion of CO under the moist condition. These results could also help to understand Au catalysis for the combustion of other organics in air.

Acknowledgement

We thank National Natural Science Foundation of China (grants: 20921001 and 20703028) for the financial support of this work.

References

[1] M. Haruta, T. Kobayashi, H. Sano, N. Yamada, Chem. Lett. (1987) 405.
[2] M. Haruta, Catal. Today 36 (1997) 153.
[3] M. Haruta, CATTECH 6 (2006) 102.
[4] M. Valden, X. Lai, D.W. Goodman, Science 281 (1998) 1647.
[5] G.C. Bond, D.T. Thompson, Gold Bull. 33 (2000) 41.
[6] G.C. Bond, C. Louis, D.T. Thompson, Catalysis by Gold, Imperial College Press, London, 2006.
[7] J.C. Fierro-Gonzalez, B.C. Gates, Catal. Today 122 (2007) 201.
[8] G.R. Bamwenda, S. Tsubota, T. Nakamura, M. Haruta, Catal. Lett. 44 (1997) 83.
[9] M. Haruta, A. Ueda, S. Tsubota, R.M. Torres Sanchez, Catal. Today 29 (1996) 443.
[10] C.B. Zhang, H. He, Catal. Today 126 (2007) 345.
[11] J.D. Grunwaldt, C. Kiener, C. Wogerbauer, A. Baiker, J. Catal. 181 (1999) 223.
[12] P. Claus, A. Bruckner, C. Mohr, H. Hofmeister, J. Am. Chem. Soc. 122 (2000) 11430.
[13] D. Andreeva, T. Tabakova, L. Ilieva, A. Naydenov, D. Mehanjiev, M.V. Abrashev, Appl. Catal. A: Gen. 209 (2001) 291.
[14] X. Zhang, H. Wang, B.Q. Xu, J. Phys. Chem. B 109 (2005) 9678.
[15] J.H. Yang, J.D. Henao, M.C. Raphulu, Y.M. Wang, T. Caputo, A.J. Groszek, M.C. Kung, M.S. Scurrell, J.T. Miller, H.H. Kung, J. Phys. Chem. B 109 (2005) 10319.
[16] X. Zhang, H. Shi, B.Q. Xu, Angew. Chem. Int. Ed. 44 (2005) 7132.
[17] X. Zhang, H. Shi, B.Q. Xu, Catal. Today 122 (2007) 330.
[18] Y. Wu, K.Q. Sun, J. Yu, B.Q. Xu, Phys. Chem. Chem. Phys. 10 (2008) 6399.
[19] D.P. He, H. Shi, Y. Wu, B.Q. Xu, Green Chem. 9 (2007) 849.
[20] B.Q. Xu, J.M. Wei, Y.T. Yu, J.L. Li, Q.M. Zhu, Top. Catal. 22 (2003) 77.
[21] Z.L. Wu, S.H. Zhou, H.G. Zhu, S. Dai, S.H. Overbury, Chem. Commun. (2008) 3308.
[22] M.J. Li, Z.L. Wu, Z. Ma, V. Schwartz, D.R. Mullins, S. Dai, S.H. Overbury, J. Catal. 266 (2009) 98.
[23] Z.L. Wu, S.H. Zhou, H.G. Zhu, S. Dai, S.H. Overbury, J. Phys. Chem. C 113 (2009) 3726.
[24] F. Boccuzzi, A. Chiorino, S. Tsubota, M. Haruta, J. Phys. Chem. 100 (1996) 3625.
[25] M. Date, M. Haruta, J. Catal. 201 (2001) 221.
[26] M. Date, M. Okumura, S. Tsubota, M. Haruta, Angew. Chem. Int. Ed. 43 (2004) 2129.
[27] R. Zanella, S. Giorgio, C.R. Henry, C. Louis, J. Phys. Chem. B 106 (2002) 7634.
[28] T. Salthammer, S. Mentese, R. Marutzky, Chem. Rev. 110 (2010) 2536.
[29] M.L. Jia, Y.N. Shen, C.Y. Li, Z. Bao, S.S. Sheng, Catal. Lett. 99 (2005) 235.
[30] Y.N. Shen, X.Z. Yang, Y.Z. Wang, Y.B. Zhang, H.Y. Zhu, L. Gao, M.L. Jia, Appl. Catal. B: Environ. 79 (2008) 142.
[31] C.Y. Li, Y.N. Shen, M.L. Jia, S.S. Sheng, M.O. Adebajo, H.Y. Zhu, Catal. Commun. 9 (2008) 355.
[32] X.Z. Yang, Y.N. Shen, D.H. Wang, Y.A. Sun, React. Kinet. Catal. Lett. 95 (2008) 123.
[33] J.L. Jia, D.H. Wang, J.J. Jin, Z.Y. Zhang, X.C. Shi, J. Beijing Univ. Chem. Technol. 35 (2008) 1.
[34] J.J. Jin, X.C. Shi, D.H. Wang, J. Jia, L. Lv, Z.Y. Zhang, J.S. Jin, J. Beijing Univ. Chem. Technol. 36 (2009) 20.
[35] N. Ta, Y.N. Shen, C. Wang, Y.B. Zhang, Qiherima, Acta Sci. Circumstan. 29 (2009) 1164.
[36] J. Zhang, Y. Jin, C.Y. Li, Y.N. Shen, L. Han, Z.X. Hu, X.W. Di, Z.L. Liu, Appl. Catal. B: Environ. 91 (2009) 11.
[37] Y.B. Zhang, Y.N. Shen, X.Z. Yang, S.S. Sheng, T.N. Wang, M.F. Adebajo, H.Y. Zhu, J. Mol. Catal. A: Chem. 316 (2010) 100.